Wagner, G., & Wüthrich, K. (1982) *J. Mol. Biol. 155*, 347.
Wagner, G., Neuhaus, D., Wörgötter, E., Vasak, M., Kagi, J. H. R., & Wüthrich, K. (1986) *J. Mol. Biol. 187*, 131.
Wider, G., Lee, K. H., & Wüthrich, K. (1982) *J. Mol. Biol. 155*, 367.
Wider, G., Macura, S., Kumar, A., Ernst, R. R., & Wüthrich, K. (1984) *J. Magn. Reson. 56*, 207.
Wilner, G. D., Nossel, H. L., Canfield, R. E., & Butler, V. P., Jr. (1976) *Biochemistry 15*, 1209.
Wilner, G. D., Thomas, D. W., Nossel, H. L., Robbins, P. F., & Mudd, M. S. (1979) *Biochemistry 18*, 5078.
Wüthrich, K. (1986) *NMR of Proteins and Nucleic Acids*, Wiley, New York.
Wüthrich, K., Wider, G., Wagner, G., & Braun, W. (1982) *J. Mol. Biol. 155*, 311.
Wüthrich, K., Billeter, M., & Braun, W. (1984) *J. Mol. Biol. 180*, 715.
Zimmerman, S. S., & Scheraga, H. A. (1978) *Biopolymers 17*, 1871.
Zuiderweg, E. R. P. (1987) *J. Magn. Reson. 71*, 283.

Lipid–Lipid Interactions in Reconstituted High-Density Lipoproteins by Deuterium Nuclear Magnetic Resonance†

David B. Fenske, Yashpal I. Parmar,‡ W. Dale Treleaven, Ravinder S. Chana, and Robert J. Cushley*
Department of Chemistry, Simon Fraser University, Burnaby, British Columbia, Canada V5A 1S6
Received April 24, 1987; Revised Manuscript Received February 4, 1988

ABSTRACT: Lipid–lipid interactions between the core and monolayer have been studied by using reconstituted high-density lipoproteins (rHDLs) composed of apoHDL$_3$ with either dipalmitoylphosphatidylcholine (DPPC) or egg phosphatidylcholine (egg PC) as the monolayer and either cholesteryl oleate (CO) or triolein (TO) as the core. The effect of the monolayer on the core was observed by deuterium nuclear magnetic resonance (^{2}H NMR) studies of rHDLs containing the core component cholesteryl [18,18,18-$^2H_3$]oleate ([$^2H_3$]CO) or tri[16,16-$^2H_2$]oleoylglycerol ([$^2H_6$]TO) surrounded by a monolayer of either DPPC or egg PC as a function of temperature. The reverse effect, that of the core on the monolayer, was examined by both ^{2}H and ^{31}P NMR studies of rHDLs containing [5,5-$^2H_2$]PC in the presence of CO or TO as a function of temperature. The ^{2}H NMR line widths of [$^2H_3$]CO and [$^2H_6$]TO were considerably broader and showed a greater temperature dependence in rHDLs containing DPPC than in those containing egg PC. Similarly, the C–^{2}H order parameters of [$^2H_2$]PC were higher and showed a greater temperature dependence in rHDLs containing CO than in those containing TO. In contrast, the ^{31}P NMR line widths were identical for both [$^2H_2$]-PC/CO/apoHDL$_3$ and [$^2H_2$]PC/TO/apoHDL$_3$ at 25 and 6 °C, showing only a slight temperature dependence. Thus, acyl chains of both the monolayer and core components show increased order when in contact with neighboring lipids of higher order. The data demonstrate a direct effect of core cholesteryl esters and triglycerides with the phospholipid monolayer of HDL.

Human plasma high-density lipoproteins (HDLs)[1] play an important role in both lipid transport and cholesterol homeostasis in the circulatory system (Scanu, 1979). Plasma HDL concentrations have been inversely correlated with the risk of ischemic heart disease (Miller & Miller, 1975). This antiatherogenic effect is thought to involve cholesterol efflux from the peripheral tissues (Tall & Small, 1979). The mechanism, known as reverse cholesterol transport, may proceed via esterification of HDL cholesterol by the enzyme lecithin:cholesterol acyltransferase (Tall & Small, 1979). The cholesteryl esters so produced may then be transported to the liver via HDL or transferred to the other lipoproteins by the action of lipid transfer proteins present in the plasma (Zilversmit, 1984).

The structural organization of HDLs must determine their biological roles, and thus the structure and dynamics of the lipid constituents are of considerable interest. Many techniques have been used to probe HDL structure, including electron microscopy (Forte et al., 1968), X-ray diffraction (Laggner & Muller, 1978; Baumstark et al., 1983), ESR (Brainard et al., 1980), and NMR (Finer et al., 1975; Henderson et al., 1975; Hamilton et al., 1974; Hamilton & Cordes, 1978; Wassall et al., 1982; Parmar et al., 1983). A widely accepted model of HDL structure is that of a quasi-spherical particle of 6.5–12-nm diameter (Forte et al., 1968; Scanu, 1979; Laggner & Muller, 1978) with protein, phospholipid, and cholesterol in an outer monolayer and cholesteryl esters and triglyceride in a hydrophobic core (Smith et al., 1978). There is considerable debate, however, regarding the organization

† This work was supported by the British Columbia Heart Foundation.
* Author to whom correspondence should be addressed.
‡ Present address: Shaughnessy Hospital Research Center, University of British Columbia, 950 West 28th Ave., Vancouver, British Columbia, Canada V5Z 4H4.

[1] Abbreviations: rHDL, reconstituted high-density lipoprotein; ^{2}H NMR, deuterium nuclear magnetic resonance; ^{31}P NMR, phosphorus-31 nuclear magnetic resonance; DSC, differential scanning calorimetry; [$^2H_3$]CO, cholesteryl [18,18,18-$^2H_3$]oleate; [$^2H_2$]PC, phosphatidylcholine synthesized from egg L-α-lysophosphatidylcholine and [5,5-$^2H_2$]palmitic acid; [$^2H_{31}$]PC, phosphatidylcholine synthesized from egg L-α-lysophosphatidylcholine and [$^2H_{31}$]palmitic acid; [$^2H_6$]TO, tri[16,16-$^2H_2$]-oleoylglycerol; egg PC, egg phosphatidylcholine; DPPC, dipalmitoylphosphatidylcholine; TO, triolein; CO, cholesteryl oleate; apoHDL$_3$, apoproteins isolated from HDL$_3$; ESR, electron spin resonance; TLC, thin-layer chromatography; SDS, sodium dodecyl sulfate.

0006-2960/88/0427-4491$01.50/0

of the neutral core lipids, with some groups (Hamilton & Cordes, 1978; Shen et al., 1977) proposing the existence of a separate domain of cholesteryl ester and triglyceride and others (Laggner & Muller, 1978; Baumstark et al., 1983; Verdery & Nichols, 1975) proposing interdigitation of core components with the phospholipid acyl chains.

Deuterium NMR is an excellent technique for studying molecular order (organization) and dynamics as it monitors a nonperturbing probe. The technique has recently been applied to the study of deuteriated cholesteryl esters in native LDL (Treleaven et al., 1986) and rHDL (Parmar et al., 1983). The use of rHDL particles provides a means of placing deuterium probes at almost any position within the lipoprotein complex, thereby allowing selective information on lipid motions and organization to be monitored. In the present paper, we report results of studies on the two major regions of the rHDL particle. First, the effect of the monolayer on the core was studied by comparing the ^2H NMR spectra of rHDLs containing a core of [$^2H_3$]CO or [$^2H_6$]TO surrounded by a monolayer of either egg PC or DPPC. Second, the effect of the core on the monolayer was studied by comparing the ^2H and ^{31}P NMR spectra of rHDLs containing [$^2H_2$]PC in the monolayer and either CO or TO in the core.

The question of interest was whether varying the order of either core or monolayer would affect the order of the neighboring domain, thereby providing evidence for communication between these two regions of the lipoprotein complex, thus shedding light on core–monolayer organization.

Materials and Methods

[18,18,18-$^2H_3$]Oleic acid and [5,5-$^2H_2$]palmitic acid were generous gifts from the late Dr. A. P. Tulloch, Plant Biochemistry Institute, National Research Council of Canada, Saskatoon, Saskatchewan. [$^2H_6$]TO was a generous gift from Dr. H. Gorrissen, presently at BASF AG, Abt. Kunststofflabor, D-6700, Ludwigshafen, FRG. Egg lysophosphatidylcholine and deuterium-depleted water were purchased from Sigma Chemical Co. Sigma lysophosphatidylcholine contains 66–68% palmitic acid, 24–26% stearic acid, and 6–10% other saturated acids. Cholesterol was obtained from Fisher Scientific Co. and was recrystallized 3 times from benzene.

Synthesis of [$^2H_3$]CO, [$^2H_2$]PC, and [$^2H_{31}$]PC. Cholesteryl [18,18,18-$^2H_3$]oleate ([$^2H_3$]CO) was synthesized from cholesterol and [18,18,18-$^2H_3$]oleic acid as reported by Treleaven et al. (1986). The details of the melting point and mass spectral analysis of [$^2H_3$]CO have been reported (Treleaven et al., 1986).

[5,5-$^2H_2$]Phosphatidylcholine ([$^2H_2$]PC) and [$^2H_{31}$]phosphatidylcholine ([$^2H_{31}$]PC) were synthesized by condensation of [5,5-$^2H_2$]palmitic acid and [$^2H_{31}$]palmitic acid, respectively, to the *sn*-2 position of egg L-α-lysophosphatidylcholine using 1,1′-carbonyldiimidazole (Thewalt et al., 1985). The [$^2H_2$]PC showed a single spot on silica gel TLC plates when run in $CHCl_3/CH_3OH/H_2O$ (65:25:4). The DSC of multilamellar dispersions of [$^2H_2$]PC showed a pretransition at 32 °C and a phase transition at 42 °C. The values for [$^2H_{31}$]PC were 31 and 40 °C, respectively (Thewalt et al., 1985).

Isolation of ApoHDL$_3$. Native HDL$_3$ was isolated from fresh (<3 days old) human plasma by ultracentrifugal floatation in the density range 1.125–1.210 g mL^{-1} (Havel et al., 1955). The HDL$_3$ from several units was pooled and purified by reisolation in the same density range. ApoHDL$_3$ was isolated by using the technique of Scanu et al. (1969).

Preparation of rHDL. Reconstituted HDL particles were prepared by the established procedure of Hirz and Scanu (1970). For the [$^2H_3$]CO/DPPC(egg PC) and [$^2H_2$]PC/CO(TO) rHDLs, 18 mg of core component ([$^2H_3$]CO, CO, or TO) was codissolved in chloroform with 27 mg of egg PC, DPPC, or [$^2H_2$]PC. The chloroform was removed under a stream of N_2, and the lipids were placed under high vaccuum overnight. A lipid–water emulsion was formed by mixing the lipids with approximately 6 mL of deuterium-depleted water at 50 °C. ApoHDL$_3$ (55 mg) was added to the mixture as a solid and gently stirred until dissolved. When a homogeneous dispersion was obtained, the mixture was sonicated, under nitrogen, until translucent using a Heat Systems W-375 sonicator operating at 35–40% output power. The sonication time varied from 6 to 30 min, using 1.5-min pulses followed by 2-min cooling periods. The temperature in the vessel was maintained at 48–52 °C (near the isotropic melt of CO). The temperature was monitored by inserting a thermocouple directly into the sonication mixture. Titanium particles were removed by centrifugation on a clinical centrifuge followed by filtration (Gelman Acrodisc polysulfone filters; 0.2 μm). The preparation of [$^2H_{31}$]PC/TO rHDL was identical except that the amount of starting materials was increased slightly (60 mg of protein, 30 mg of [$^2H_{31}$]PC, and 20 mg of TO).

[$^2H_6$]TO/DPPC(egg PC) rHDLs of mean diameter $\simeq$13 nm were prepared as described above except that the amount of starting material was reduced (25 mg of protein, 12.3 mg of DPPC or egg PC, and 8.2 mg of [$^2H_6$]TO), and the lipid–protein emulsions were sonicated for 4–6 min at 37 °C on a Biosonics sonicator, using 2-min pulses followed by 1-min cooling periods. These particles were reduced in size to $\simeq$11-nm diameter by sonication for 10 min at 37–47 °C ([$^2H_6$]TO/egg PC/apoHDL$_3$) or 46–50 °C ([$^2H_6$]TO/DPPC/apoHDL$_3$) on a Heat Systems W-375 sonicator operating at $\simeq$35% output power; 1- or 2-min pulses were used, followed by 2-min cooling periods.

rHDL was isolated in the density range 1.125–1.210 g mL^{-1}. Density adjustments were performed by using solid KBr or a saturated KBr solution prepared in deuterium-depleted water. The samples were run as isolated, in $\simeq$2 M KBr. In order to determine the solvent viscosities, a solution of KBr (1.21 g/mL) was centrifuged under identical conditions as the rHDL samples, and an aliquot equal in volume to the rHDL samples was removed. Solvent viscosities (η) as a function of temperature were determined over the temperature range 2–48 °C using an Ostwald viscometer. Viscosity values below 0 °C were obtained by extrapolation of a plot of log η vs $1/T$.

Protein was determined by the method of Lowry et al. (1951) and phospholipid by the method of Ames (1966). Cholesteryl ester and triglyceride were determined enzymatically by the use of Boehringer Mannheim clinical test kits. The estimated error in these analyses, based on duplicate runs on the same sample, was ±2% for protein and phospholipid and ±10% for cholesteryl ester and triglyceride.

Gel Electrophoresis. The integrity of apoHDL$_3$ following isolation and sonication was verified by SDS–polyacrylamide gel electrophoresis using the methodology of Laemmli (1970). The concentrations of polyacrylamide in the stacking and separating gels were 4% and 10%, respectively. The gels were stained with Coomassie brilliant blue R 250.

Electron Microscopy. The size distribution of the rHDL particles was determined by negative-staining electron microscopy with a Philips 300 electron microscope operating at 80 kV, using 2% ammonium molybdate, pH 8.6, on 200-mesh Formvar carbon-coated grids. The rHDL was dialyzed against phosphate-buffered saline, pH 7.4, prior to the negative-staining procedure. Typically, 0.5 mg of protein/mL rHDL particles was deposited on the grid and allowed to stand for

$\simeq$2 min. The excess fluid was desorbed by using Whatman filter paper. The stain solution was immediately applied and also removed after 2 min. The particle diameters were measured directly from the negative or by projecting the negative image onto a screen.

Nuclear Magnetic Resonance. The ^2H NMR experiments were performed at 38.8 MHz with a home-built spectrometer and a 5.9-T Nalorac superconducting magnet interfaced to a Nicolet BNC-12 computer or a Vax Workstation I. Temperatures were controlled by a solid-state temperature controller with an accuracy of ±0.25 °C built by the Simon Fraser University electronics shop. High-resolution spectra were obtained by using a one-pulse sequence with phase alternation in order to minimize base-line distortion. The [$^2H_3$]CO rHDL spectra were obtained by using a spinning probe while all other spectra were obtained on a broad-band probe with a horizontally mounted coil. The samples were allowed to equilibrate for 30 min at a given temperature before acquiring data. The spectral parameters are given in the figure legends. Longitudinal relaxation times, T_1, were measured at 38.8 MHz by the inversion–recovery method $(180°-\tau-90°-T)_n$, where signal intensities (A) were used to obtain T_1 from the expression $A_\tau = A_\infty(1 - 2e^{-\tau/T_1})$. The delay time T was 0.1 s for the [$^2H_2$]PC rHDLs at 25 °C and 0.26 and 0.20 s for the [$^2H_6$]TO rHDLs at 25 and −5 °C, respectively.

^2H NMR powder spectra of neat [$^2H_3$]CO (not shown) were obtained by using the quadrupolar echo pulse sequence $(90°|_{0°}-\tau-90°|_{90°}-T)_n$. Data collection was accomplished with an Explorer IIIA digital oscilloscope while Fourier transformation was performed by using a Nicolet BNC-12 computer. The spectra were symmetrized by zeroing the out-of-phase quadrature channel and reflecting the spectrum about the central (carrier) frequency. This results in an improvement in S/N by $\sqrt{2}$.

The ^2H spectra shown in Figures 2, 4, and 6 were analyzed by using a seven-parameter iterative least-squares fit of the ^2HOH and [$^2H_3$]CO (Figure 2), [$^2H_6$]TO (Figure 4), or [$^2H_2$]PC (Figure 6) resonances to Lorentzian functions. Spectra of [$^2H_{31}$]PC/TO/apoHDL$_3$ in the presence of 2 M KBr and in deuterium-depleted water (not shown) were analyzed by using a six-parameter fit to three Lorentzian functions. These functions were chosen to approximate high- and low-order methylene segments and the terminal methyl group. The areas under the three Lorentzians were constrained in the ratio 14:14:3, and the C^2H_3 chemical shift was offset 15 Hz upfield from that of the C^2H_2. The program was kindly provided by Dr. K. E. Newman, Chemistry Department, Simon Fraser University, and was run by using an IBM 3081 GX computer in the Computing Services Department of Simon Fraser University.

The ^{31}P NMR experiments were performed at 102.2 MHz, without proton decoupling, on the home-built spectrometer, using the broad-band probe. The ^{31}P spectra (not shown) were analyzed by using a four-parameter fit to a single Lorentzian function.

Theory

The ^2H quadrupolar splitting of a C–^2H bond in a single crystal is given by (Abragam, 1961a)

$$\Delta\nu = (3/2)(e^2qQ/h)[(3\cos^2\theta - 1)/2 + (\eta\sin^2\theta\cos 2\phi)/2] \quad (1)$$

where θ and ϕ define the relative orientation of the C–^2H vector with respect to the external magnetic field B_0. A dry, polycrystalline sample of [$^2H_3$]CO or [$^2H_2$]PC yields a ^2H NMR powder pattern spectrum which results from the superposition of splittings $\Delta\nu$ for all orientations of the C–^2H bond with respect to B_0. For [$^2H_2$]PC, the asymmetry parameter η is known to be $\simeq$0 (Burnett & Muller, 1971), and we assume the same for [$^2H_3$]CO by analogy with the closely related compound cholesteryl [16,16,16-$^2H_3$]palmitate (Valic et al., 1979). The splittings of the two most intense peaks in the powder spectrum, the characteristic Pake doublet splitting $\Delta\nu_Q$, occur at $\theta = 90°$; hence

$$\Delta\nu_Q = (3/4)(e^2qQ/h) \quad (2)$$

where e^2qQ/h is the static quadrupolar coupling constant, taken to be 170 kHz for a C^2H_3 or C^2H_2 alkane group (Burnett & Muller, 1971).

Fast, anisotropic motions of the C^2H_3 and C^2H_2 occur about the molecular long axis (director) and will reduce $\Delta\nu_Q$ from its static value. In the case of C^2H_3, one must first consider fast methyl group rotation which reduces $\Delta\nu_Q$ to 38 kHz (Burnett & Muller, 1971). Second, fast chain isomerizations and possibly director "tilting" lead to random fluctuations of the C–^2H bond, resulting in a reduction of $\Delta\nu_Q$ to a residual splitting $\Delta\nu_r$ given by

$$\Delta\nu_r = (3/4)(e^2qQ/h)S_{CD} \quad (3)$$

where the C–^2H bond order parameter S_{CD} is given by

$$S_{CD} = \langle 3\cos^2\beta - 1\rangle/2 \quad (4)$$

where β is the angle the C–^2H bond makes with the director and the angular brackets denote an average over time (time scale 10^{-5} s or longer).

Isotropic motions (e.g., tumbling of the lipoprotein particle) further reduce $\Delta\nu_Q$ to a single Lorentzian signal. This reduction is most conveniently seen from consideration of the second moment of the powder pattern. The second moment M_2 has the general form

$$M_2 = \int_{-\infty}^{\infty}\omega^2 f(\omega)\,d\omega \Big/ \int_{-\infty}^{\infty} f(\omega)\,d\omega \quad (5)$$

where $f(\omega)$ is the intensity of the powder pattern at frequency ω from the center of the Pake doublet. The line width at half-height ($\Delta\nu_{1/2}$) for the Lorentzian line is related to M_2 by (Abragam, 1961b)

$$\pi\Delta\nu_{1/2} = M_2\tau_e + C \quad (6)$$

where C is a constant containing contributions from τ_e-independent processes, such as magnetic field inhomogeneity and spin–lattice relaxation. In the present case, the value of the natural line width of deuterium oxide was used (C = 2.5 Hz). The effective correlation time τ_e is given by

$$1/\tau_e = 1/\tau_t + 1/\tau_d \quad (7)$$

where τ_t is the correlation time for particle tumbling and τ_d is the correlation time for phospholipid lateral diffusion in the HDL monolayer. These are given by

$$\tau_t = 4\pi\eta R^3/3kT \quad (8)$$

$$\tau_d = R^2/6D \quad (9)$$

where η is the solvent viscosity, R is the particle radius, k is the Boltzmann constant, and D is the lateral diffusion coefficient for phospholipids in the HDL monolayer. M_2 is also related to the quadrupolar splitting $\Delta\nu_Q$ by

$$M_2 = (4/5)\pi^2\Delta\nu_Q^2 \quad (10)$$

For C^2H_2 groups, the static quadrupolar splitting $\Delta\nu_Q$ in eq 10 is $\simeq$126 kHz (Burnett & Muller, 1971). Fast, anisotropic

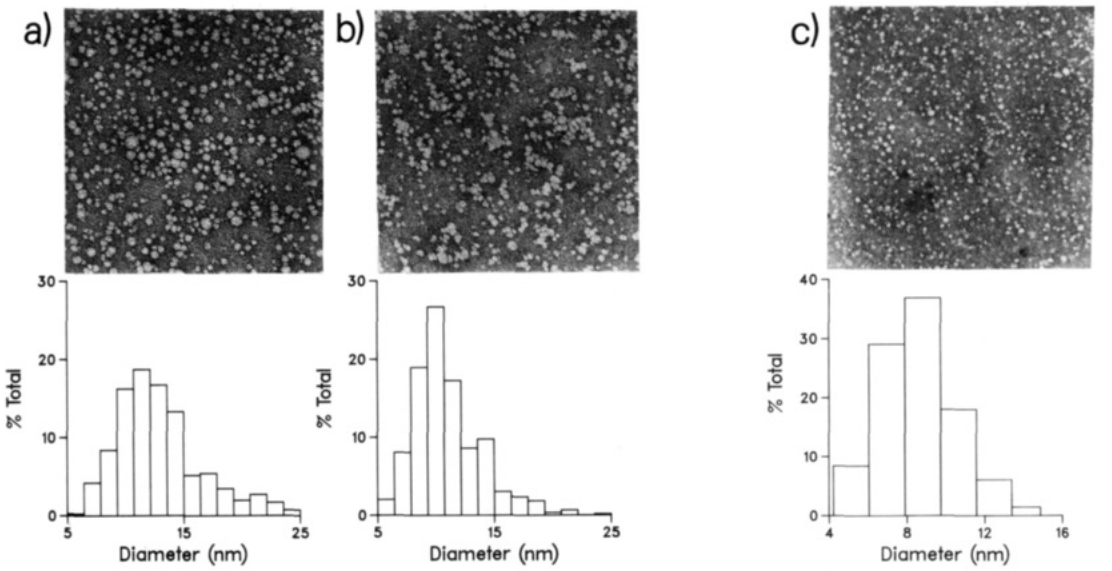

FIGURE 1: Representative electron micrographs and histograms of the size distributions of (a) $[^2H_6]$TO/egg PC/apoHDL$_3$ (diameter = 13 nm) (magnification = 78750×), (b) $[^2H_6]$TO/DPPC/apoHDL$_3$ (diameter = 11 nm) (magnification = 77850×), and (c) $[^2H_2]$PC/CO/apoHDL$_3$ (magnification = 58500×).

acyl chain reorientations reduce the second moment from its rigid lattice value to a residual second moment M_{2_r}. Under the assumption that the rate of local molecular reorientations is much faster than the isotropic motions described by τ_e, the line width may be expressed by

$$\pi\Delta\nu_{1/2} = M_{2_r}\tau_e + 1/T_1 \quad (11)$$

where $1/T_1$ is the spin–lattice relaxation rate. This equation does not allow for the possibility of slow anisotropic motions being present. Assuming that the molecular motions within the HDL monolayer are axially symmetric about the normal to the particle surface, i.e., the radial direction (as found for phospholipids in unilamellar vesicles), we can write

$$M_{2_r} = (4/5)\pi^2\Delta\nu_r^2 \quad (12)$$

where $\Delta\nu_r$ is given by

$$\Delta\nu_r = (3/4)(e^2qQ/h)S_{CD} \quad (13)$$

Substitution of eq 12 and 13 into eq 11 yields (Stockton et al., 1976)

$$\Delta\nu_{1/2} = (9\pi/20)(e^2qQ/h)^2S_{CD}^2\tau_e + 1/\pi T_1 \quad (14)$$

RESULTS

Three comparative studies have been performed using six different rHDLs. These may be summarized as follows: (1) $[^2H_3]$CO/DPPC/apoHDL$_3$ and $[^2H_3]$CO/egg PC/apoHDL$_3$; (2) two different sizes of both $[^2H_6]$TO/DPPC/apoHDL$_3$ and $[^2H_6]$TO/egg PC/apoHDL$_3$; (3) $[^2H_2]$PC/CO/apoHDL$_3$ and $[^2H_2]$PC/TO/apoHDL$_3$.

In order for the results obtained to be directly comparable, it is necessary that the reconstituted particles within each study have similar mean diameter and chemical composition. This was demonstrated by determining the size distributions using electron microscopy and the particle compositions by chemical analysis. Figure 1 shows representative electron micrographs of $[^2H_6]$TO/egg PC/apoHDL$_3$ (diameter = 13.1 nm), $[^2H_6]$TO/DPPC/apoHDL$_3$ (diameter = 11.0 nm), and $[^2H_2]$PC/CO/apoHDL$_3$ (diameter = 8.7 nm). The particles look uniform in size and are spherical, as in the case of native HDL. The size distributions are shown beneath the micrographs and were obtained from several different field measurements in each case. The mean diameters of the $[^2H_6]$-TO/DPPC/apoHDL$_3$ and $[^2H_6]$TO/egg PC/apoHDL$_3$ were 13.2 ± 4.3 and 13.1 ± 4.0 nm, respectively. Following a second sonication, these sizes were reduced to 11.0 ± 3.1 and 11.2 ± 3.2 nm, respectively. The larger size of these particles is reflected in the increased percentage of core components (25% as compared with ≃15% in the other rHDLs). The mean diameters of the $[^2H_2]$PC/CO/apoHDL$_3$ and $[^2H_2]$PC/TO/apoHDL$_3$ were 8.7 ± 2.0 and 9.1 ± 1.9 nm (Table I), with 56% and 57% of the particles falling in the 7.3–9.5-nm size range, respectively. The mean diameters of $[^2H_3]$CO/DPPC/apoHDL$_3$ and $[^2H_3]$CO/egg PC/apoHDL$_3$ were 9.0 ± 1.6 and 8.7 ± 1.6 nm, respectively (Table I), and in both cases, 64% of the particles fell in the 7.3–9.4-nm size range. The values for the $[^2H_3]$CO and $[^2H_2]$PC rHDLs are only slightly larger than those determined for the native HDL$_3$ from which the protein was isolated (mean diameter of 8.1 ± 1.6 nm with 62% of the particles in the range 7.2–9.3 nm). Additionally, each pair of rHDLs within a given study has es-

Table I: Physical Parameters of rHDLs Reconstituted from ApoHDL$_3$ and the Indicated Lipid Mixtures, Isolated in the Density Range 1.125–1.21 g/mL

	$[^2H_3]$CO/ DPPC	$[^2H_3]$CO/ egg PC	$[^2H_2]$PC/ CO	$[^2H_2]$PC/ TO
diameter[a] (nm)	9.0 (±1.6)[b]	8.7 (±1.6)	8.7 (±2.0)	9.1 (±1.9)
comp (wt %)				
protein	46	46	53	53
PC	38	39	32	31
CO	16	15	15	
TO				16
T_1 (ms)[c]			16	14
	$[^2H_6]$TO/ DPPC	$[^2H_6]$TO/ egg PC	$[^2H_6]$TO/ DPPC	$[^2H_6]$TO/ egg PC
diameter[a] (nm)	13.2 (±4.3)	13.1 (±4.0)	11.0 (±3.1)	11.2 (±3.2)
comp (wt %)				
protein	53	54	55	56
PC	22	21	19	19
TO	25	25	26	25
T_1 (ms)[c]	17 (−5 °C) 33 (25 °C)	19 (−5 °C) 34 (25 °C)		

[a] Mean diameter from electron microscopy measurements; between 200 and 600 particles were measured for each sample. [b] The number in parentheses represents the standard deviation. [c] Deuterium spin–lattice relaxation time of the deuteriated lipid measured at 25 °C or as indicated.

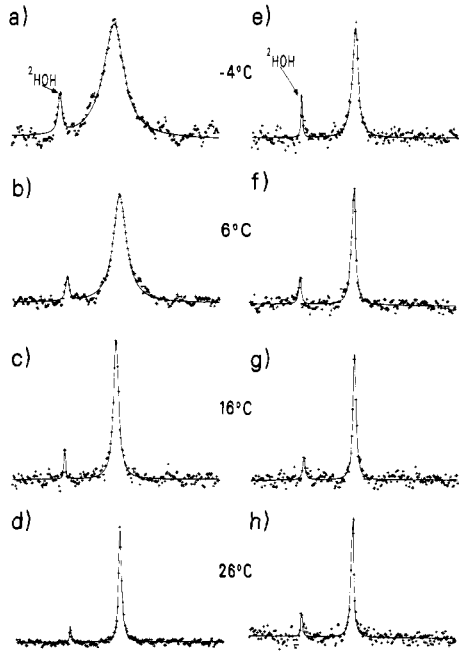

FIGURE 2: ^2H NMR spectra of $[^2H_3]CO$ in HDL reconstituted with either DPPC (a–d) or egg PC (e–h) as a function of temperature. The plot width is 600 Hz in all cases. The solid line represents an iterative least-squares fit to the data points (crosses). For illustrative purposes, every third data point is plotted. Spectral parameters: pulse width = 20 μs (flip angle = 90°); sweep width = 1 kHz; number of acquisitions = 4021 (a), 2936 (b), 2048 (c, d), 2942 (e), 2208 (f), 2182 (g), and 1457 (h); data sets = 2K (a–g) and 4K (h); delay between pulses = 1.1 s (a–g) and 2.1 s (h); line broadening = 5 Hz (a, b) and 2 Hz (c–h); delay before acquisition = 10 μs.

sentially identical chemical composition (Table I). Thus, the only major difference between the two $[^2H_3]CO$ rHDLs and the $[^2H_6]TO$ rHDLs lies in the fatty acyl chain composition of the phospholipid monolayer. Likewise, the two $[^2H_2]PC$ rHDLs differ only in their core lipids. The average size of the $[^2H_3]CO$ and $[^2H_2]PC$ rHDLs and the chemical composition of the $[^2H_3]CO$ rHDLs lie between the literature values for HDL_2 and HDL_3. The chemical composition of the $[^2H_2]PC$ rHDLs is closer to that of HDL_3. The $[^2H_6]TO$ rHDLs are in the size range of HDL_2. Although simpler in composition than the native particles, the rHDLs are good models of the native systems as far as size, relative proportion of core/monolayer components, and ^2H NMR parameters (see Discussion) are concerned.

It has been shown by circular dichroism measurements that the conformation of $apoHDL_3$ is identical in native and reconstituted particles (Hirz & Scanu, 1970) and that sonication of apo A-I does not result in structural changes of the apoprotein (Ritter & Scanu, 1977). The integrity of apo A-I after sonication has also been demonstrated by immunodiffusion, electrophoresis, and amino acid analysis (Ritter & Scanu, 1977). In order to ensure that the sonication conditions used in the present study did not damage the apoproteins, we have used SDS–polyacrylamide gel electrophoresis to compare the proteins of native HDL_3 and isolated $apoHDL_3$ with those of a sample of $apoHDL_3$/egg PC/cholesterol (24:72:4 by weight) sonicated for 30 min as described above. This represents the maximum sonication time employed in our study, and no evidence of protein degradation was observed.

Effect of Monolayer on Core. Results with $[^2H_3]CO$. Representative ^2H NMR spectra of rHDL containing $[^2H_3]CO$ and either egg PC or DPPC as the surrounding monolayer are shown in Figure 2 as a function of temperature. In addition to the signal observed from the $[^2H_3]CO$, the

Table II: Temperature-Dependent ^2H NMR Line Widths[a] of $[^2H_3]CO$ and $[^2H_6]TO$ in rHDL Containing either DPPC or Egg PC

	$\Delta\nu_{1/2} - C$ (Hz)			
T (°C)	$[^2H_3]CO$/ DPPC	$[^2H_3]CO$/ egg PC	$[^2H_6]TO$/ DPPC[b]	$[^2H_6]TO$/ egg PC[b]
−8.0	71			
−5.0			154	70
−4.0	64 (65)[c]	15 (16)[c]		
−2.3	57			
−2.0		13		
0.0	60			
1.0	50	12		
3.5	40			
5.0			78	45
6.0	38 (38)	9.2 (9.5)		
11.0	24	8.3		
15.0			45	34
16.0	13 (13)	6.5 (6.3)		
18.0	13			
20.0			33	
21.0	9.2			
25.0			26	24
26.0	5.9 (5.9)	4.3 (4.8)		
35.0			20	18
45.0			14	13

[a] The line widths for the $[^2H_6]TO$ rHDLs were obtained from an iterative least-squares fit of the $[^2H_6]TO$ resonance. Measured line widths are accurate to ±10%. The constant C = 2.5 Hz is defined under Theory. [b] The mean diameters were 13.2 ± 4.3 and 13.1 ± 4.0 nm for the $[^2H_6]TO$/DPPC/$apoHDL_3$ and $[^2H_6]TO$/egg PC/$apoHDL_3$ rHDLs, respectively. [c] The numbers in parentheses represent the line width obtained from an iterative least-squares fit of the $[^2H_3]CO$ resonance.

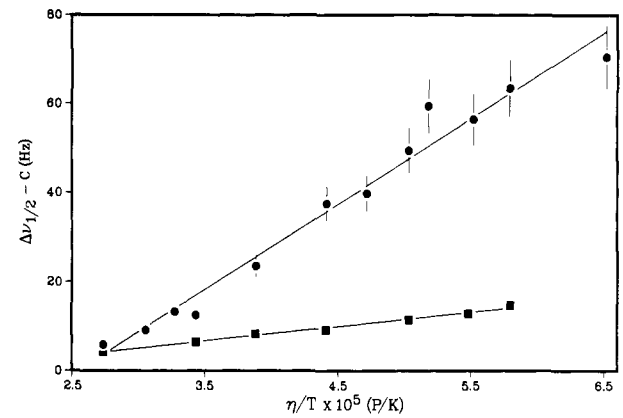

FIGURE 3: ^2H NMR line widths ($\Delta\nu_{1/2}$) of $[^2H_3]CO$ in rHDL containing either DPPC (circles) or egg PC (squares) as a function of η/T. The error bars represent an estimated uncertainty in the line widths of ±10%.

spectra also contain a narrow resonance, ≃145 Hz downfield, due to the residual deuterium in water. The signals are simulated by single Lorentzian line-shape functions. The temperature dependence of the ^2H NMR line widths ($\Delta\nu_{1/2}$) for the two samples is given in Table II. The line widths obtained are independent of whether the sample was heated or cooled over the temperature range studied. The samples do not freeze even at −8.0 °C due to the presence of ≃2 M KBr, which depresses the freezing point of water by ≃8 °C. The observed line widths are shown in Figure 3 as a function of η/T. The temperature dependence is more pronounced for $[^2H_3]CO$/DPPC/$apoHDL_3$ (slope = 1.93 × 10^6 K·P^{-1}·s^{-1}) than for $[^2H_3]CO$/egg PC/$apoHDL_3$ (slope = 3.37 × 10^5 K·P^{-1}·s^{-1}). The two curves are linear with correlation coefficients of 0.987 and 0.995, respectively.

Effect of Monolayer on Core. Results with $[^2H_6]TO$. Representative ^2H NMR spectra of rHDLs (diameter 13 nm) containing $[^2H_6]TO$ as the core component and either DPPC

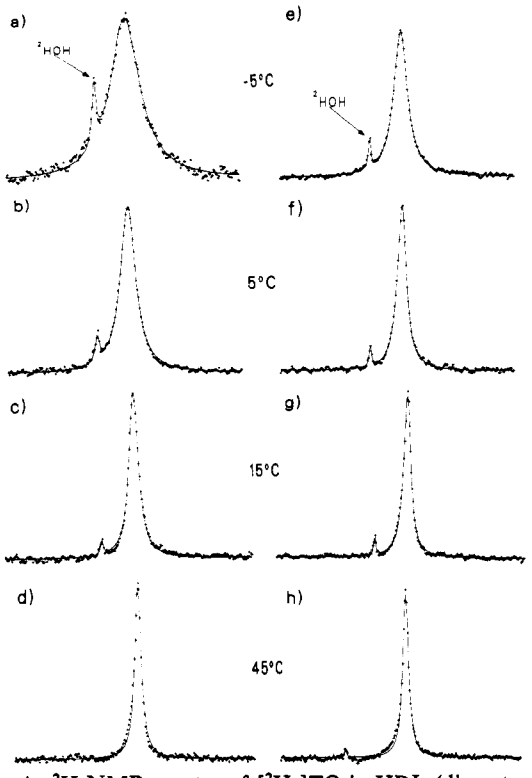

FIGURE 4: ^{2}H NMR spectra of [$^2H_6$]TO in HDL (diameter = 13 nm) reconstituted with either DPPC (a–d) or egg PC (e–h) as a function of temperature. The plot width is 1013 Hz in (a–c) and (e–g) and 500 Hz in (d) and (h). The solid line represents an iterative least-squares fit to the data points (crosses). Spectral parameters: pulse width = 8 μs (flip angle = 90°); sweep width = 5 kHz (a, b, e, and f) and 2 kHz (c, d, g, and h); number of acquisitions = 16 069 (a), 18 617 (b), 12 000 (c), 7700 (d), 15 300 (e), 9043 (f), 13 014 (g), and 10 877 (h); data sets = 2K (a, b, e, and f) and 1K zero-filled to 2K (d, h) and 1K (c, g); delay between pulses = 0.20 s (a, b, e, and f) and 0.26 s (c, d, g, and h); line broadening = 5 Hz (a, b, e, and f), 4 Hz (c, g), and 1 Hz (d, h); delay before acquisition = 10 μs.

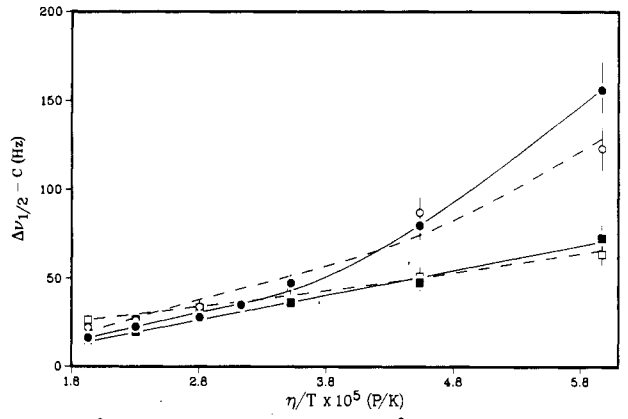

FIGURE 5: ^{2}H NMR line widths ($\Delta\nu_{1/2}$) of [$^2H_6$]TO rHDL containing either DPPC (circles) or egg PC (squares) as a function of η/T. The solid lines represent 13-nm [$^2H_6$]TO/DPPC/apoHDL$_3$ (closed circles) and [$^2H_6$]TO/egg PC/apoHDL$_3$ (closed squares). The dashed lines represent 11-nm [$^2H_6$]TO/DPPC/apoHDL$_3$ (open circles) and [$^2H_6$]TO/egg PC/apoHDL$_3$ (open squares). The curves are visual fits to the data points. The error bars represent an estimated uncertainty in the line widths of ±10%.

or egg PC as the surrounding monolayer are shown in Figure 4 as a function of temperature. The spectra can be simulated by single Lorentzian line-shape functions. Temperature-dependent line widths for the two samples are given in Table II. Broader line widths are observed at all temperatures for the [$^2H_6$]TO/DPPC/apoHDL$_3$, although the effect is more pronounced below 25 °C. Observed line widths are shown as a

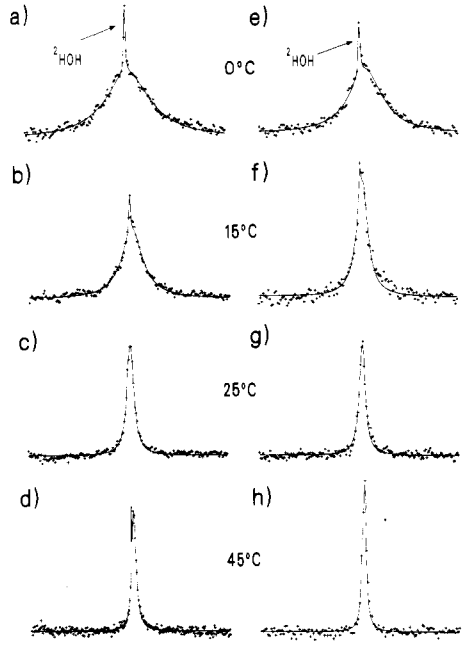

FIGURE 6: ^{2}H NMR spectra of [$^2H_2$]PC in HDL reconstituted with either CO (a–d) or TO (e–h) as a function of temperature. The plot width is 10 kHz in all cases. The solid line represents an iterative least-squares fit of Lorentzian functions to the data points (crosses). For illustrative purposes, every third (a–c, g), fourth (d–f), or eighth (h) point is plotted. Spectral parameters: pulse width = 6.5 μs (flip angle = 90°); sweep width = 10 kHz (d, h) and 20 kHz (a–c, e–g); number of acquisitions = 105 672 (a), 80 122 (b), 80 000 (c), 30 423 (d), 60 372 (e), 69 282 (f), 50 867 (g), and 35 364 (h); data sets = 2K (a–h); delay between pulses = 0.1 s (d, h) and 0.08 s (a–c, e–g); line broadening = 70 Hz (a), 60 Hz (e), 50 Hz (b), 25 Hz (f), 15 Hz (c, g), and 10 Hz (d, h); delay before acquisition = 10 μs.

function of η/T in Figure 5. Further sonication reduced the size of these particles from 13 to 11 nm, and the ^{2}H NMR line widths obtained are also given in Figure 5. The same trends are observed for the smaller particles.

^{31}P NMR spectra were obtained for the larger [$^2H_6$]TO rHDLs (13 ± 4 nm) at 25 °C, yielding line widths of 53 and 55 Hz for [$^2H_6$]TO/DPPC/apoHDL$_3$ and [$^2H_6$]TO/egg PC/apoHDL$_3$, respectively. These are the same within experimental error. As with the ^{2}H NMR spectra, the ^{31}P NMR spectra could be simulated with a single Lorentzian line-shape function.

Effect of Core on Monolayer. Representative ^{2}H NMR spectra of rHDL containing [$^2H_2$]PC and either CO or TO in the core are shown in Figure 6 as a function of temperature. The spectra can be simulated by single Lorentzian line-shape functions. Temperature-dependent line-widths for the two samples are given in Table III, along with calculated values of the C–^{2}H order parameter, S_{CD} (see Theory). A more pronounced effect is observed for [$^2H_2$]PC/CO/apoHDL$_3$ than for [$^2H_2$]PC/TO/apoHDL$_3$, with $\Delta\nu_{1/2}$ increasing from 258 to 3400 Hz as compared with 216 to 2684 Hz, respectively, as the temperature is decreased from 45 to −5 °C. A plot of S_{CD} versus T is shown in Figure 7.

^{31}P NMR line widths of rHDL containing [$^2H_2$]PC and either CO or TO are given in Table III at 25 and 6 °C. The ^{31}P NMR line widths are much less dependent on temperature than are the ^{2}H NMR line widths, increasing only 1.2-fold as compared with ≃5- and 3-fold for the ^{2}H line widths of [$^2H_2$]PC/CO/apoHDL$_3$ and [$^2H_2$]PC/TO/apoHDL$_3$, respectively, over the same temperature range.

Effect of KBr on rHDL Organization. The effect of KBr on phospholipid order in the rHDL monolayer was investigated by comparing the ^{2}H NMR spectra of [$^2H_{31}$]PC/TO/

Table III: Temperature-Dependent ^2H and ^{31}P NMR Line Widths[a] of [$^2H_2$]PC in rHDL Containing either Cholesteryl Oleate (CO) or Triolein (TO)

	CO		TO	
T (°C)	$\Delta\nu_{1/2}$ (Hz)	S_{CD}[b]	$\Delta\nu_{1/2}$ (Hz)	S_{CD}[b]
−5.0	3400	0.79	2684	0.66
0.0	2718	0.75	2036	0.61
2.5	2676	0.77		
5.0	2015	0.69		
6.0		[72][c]		[74][c]
7.5	2093	0.72	1096	0.49
8.5	1917	0.70		
12.5	1420	0.63		
15.0	1303	0.62	684	0.42
17.5	1013	0.56		
20.0	792	0.51	469	0.36
22.5	707	0.49		
25.0	418	0.39 [59]	363	0.33 [60]
27.5	365	0.37		
32.5	375	0.39	271	0.31
40.0	302	0.37	235	0.30
45.0	258	0.36	216	0.31

[a] Line widths are accurate to ±10% and were obtained from an iterative least-squares fit of the [$^2H_2$]PC resonance. [b] Calculated by using eq 14, assuming $D = 2 \times 10^{-8}$ cm^2/s. [c] The values in brackets are ^{31}P NMR line widths (hertz) obtained from an iterative least-squares fit of the ^{31}P resonance of [$^2H_2$]PC.

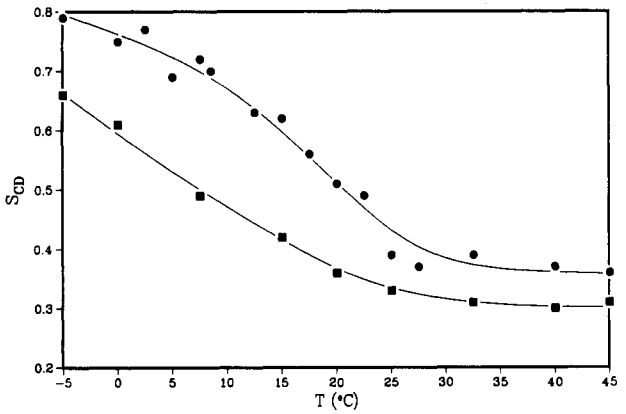

FIGURE 7: Temperature dependence of the carbon–deuterium bond order parameter S_{CD} for [$^2H_2$]PC in rHDL containing either CO (circles) or TO (squares). The curves are visual fits to the data points.

apoHDL$_3$ in 2 M KBr and in deuterium-depleted water. The resulting spectra (not shown) are super-Lorentzians resulting from the superposition of the narrow methyl resonance riding on the broader methylene resonances. The spectra were analyzed by using three Lorentzian functions to approximate the high-order methylenes (positions 2–8), the low-order methylenes (positions 9–15), and the terminal methyl group. The relative areas under the three Lorentzians were constrained in the ratio 14:14:3, respectively. When S_{CD} was calculated for each of the three regions of the perdeuteriated *sn*-2 chain, values of 0.44, 0.19, and 0.09 were obtained in the presence of 2 M KBr, and values of 0.44, 0.19, and 0.07 in its absence. Thus, no effect of KBr on the order of the monolayer could be detected.

Discussion

Effect of Monolayer on Core. An examination of the ^2H NMR spectra in Figure 2 and the data in Table II reveals that the line-width variation of [$^2H_3$]CO with temperature is highly dependent on the species of phospholipid present in each rHDL. At each temperature, the line widths of [$^2H_3$]CO/DPPC/apoHDL$_3$ are considerably broader than those of [$^2H_3$]CO/egg PC/apoHDL$_3$. Since the rHDLs have similar size and composition (Table I), the broader line widths observed for [$^2H_3$]CO/DPPC/apoHDL$_3$, compared with [$^2H_3$]CO/egg PC/apoHDL$_3$, must originate from more restricted motions of the C^2H_3 groups of the core cholesteryl esters. Several sources for this decrease in motion can be envisaged. One explanation of our results is that interdigitation of the core esters with surface phospholipid of different order influences the motions of the core esters. Over the range 0–26 °C, pure DPPC bilayers exist in the gel phase while pure egg PC bilayers are liquid-crystalline. Although phospholipids may pack differently in HDLs than in bilayers due to the small radius of curvature of the lipoproteins, it is reasonable to assume that the DPPC monolayer would still be more ordered than the egg PC monolayer at any given temperature. Thus, the [$^2H_3$]CO line widths would be broader in [$^2H_3$]CO/DPPC/apoHDL$_3$ than in [$^2H_3$]CO/egg PC/apoHDL$_3$ due to interactions with a more ordered monolayer. The difference in line widths for the ester C^2H_3 is most pronounced at lower temperatures, while at 26 °C the line widths for the two samples are nearly identical.

An alternate explanation of our results is that as the temperature decreases and the DPPC chains become more ordered, DPPC excludes the core esters from the monolayer, resulting in more restricted motions of the core esters due to packing in a smaller volume. However, there is no a priori reason why a decrease in core volume should lead to higher order, since more disarrayed packing may occur. Whatever the mechanism, it is clear that the state of the monolayer profoundly affects the neighboring core.

Plots of $\Delta\nu_{1/2}$ versus η/T for [$^2H_3$]CO in [$^2H_3$]CO/DPPC/apoHDL$_3$ and [$^2H_3$]CO/egg PC/apoHDL$_3$ are shown in Figure 3. To demonstrate that the packing is different in rHDL than it would be for neat esters, we have used eq 6 to calculate the theoretical $\Delta\nu_{1/2}$ for [$^2H_3$]CO in rHDL using the measured values of $\Delta\nu_Q$ for neat [$^2H_3$]CO at various temperatures (spectra not shown). Between −8 and 30 °C, the values of $\Delta\nu_Q$ for neat [$^2H_3$]CO remain essentially constant at $\simeq$20.7 kHz. It is only as the temperature is reduced to −39 °C that the splittings approach the theoretical maximum value of 38 kHz, thus indicating significant motion for the neat ester C^2H_3 group to low temperature. The values of the linewidths for both rHDLs are much smaller than the theoretical line widths, which demonstrates that the packing of [$^2H_3$]CO in the rHDLs is considerably different than in neat [$^2H_3$]CO. This is expected since it has been shown (Tall, 1980) that there are not enough ester molecules in HDL to form a separate ester phase. Also, the packing of esters in particles of small radius of curvature might be expected to differ from the neat phase. These two factors would be expected to result in a similar reduction of line width in both rHDLs, however, since the particle size and number of ester molecules of the two [$^2H_3$]CO rHDLs are about the same. Therefore, the large differences in slope between the [$^2H_3$]CO/DPPC/apoHDL$_3$ and [$^2H_3$]CO/egg PC/apoHDL$_3$ plots (ratio of slopes = 5.7) suggest interactions between the core and the monolayer.

In an effort to see if our observations extend to particles as large as HDL$_2$, we have made rHDLs containing [$^2H_6$]TO with mean diameters of 13 and 11 nm. Temperature-dependent ^2H NMR spectra of the 13-nm particles are shown in Figure 4, while a plot of $\Delta\nu_{1/2}$ as a function of η/T is shown in Figure 5 for both the 13- and 11-nm [$^2H_6$]TO rHDLs. As with the [$^2H_3$]CO rHDLs, the line widths were broader in both sizes of DPPC-containing rHDL than in egg PC containing rHDL at temperatures below 25 °C. Above this temperature, the line widths were the same within experimental error. While the line-width variation of the 13- and 11-nm [$^2H_6$]TO

rHDLs differs slightly, the general trends are the same. Both the size distribution and chemical composition of the 13-nm [$^2H_6$]TO/DPPC/apoHDL$_3$ and [$^2H_6$]TO/egg PC/apoHDL$_3$ are the same, and therefore the broader line widths observed for [$^2H_6$]TO/DPPC/apoHDL$_3$ at low temperatures must originate from more restricted motions of the C^2H_2 group, compared with the [$^2H_6$]TO/egg PC/apoHDL$_3$. Either of the mechanisms discussed above for [$^2H_3$]CO could account for this. The observation that the [$^2H_6$]TO line widths are broader than those of [$^2H_3$]CO at any given temperature, implying higher order in the former, is explained by noting that the CO is labeled at the methyl group of the fatty acyl chain, which gives rise to narrower line widths than do methylene positions. As well, the [$^2H_6$]TO rHDLs are significantly larger than the [$^2H_3$]CO rHDLs, which would lead to broader lines.

We assume that the effect of protein on the state of the core, if present at all, is approximately equal within each pair of [$^2H_3$]CO and [$^2H_6$]TO rHDLs, so that the differential effects we observe are attributed to phospholipid. Previous ^2H NMR studies of numerous protein–lipid systems have demonstrated a minimal effect of protein on lipid order (Bloom & Smith, 1985).

In order to determine whether the differential interactions between core component and the two monolayers had any effect on segmental reorientation rates, spin–lattice relaxation times (T_1) were determined for the large [$^2H_6$]TO rHDLs at two temperatures (Table I). At −5 °C, where the line-width differences are largest, values of 17 and 19 ms were obtained for [$^2H_6$]TO/DPPC/apoHDL$_3$ and [$^2H_6$]TO/egg PC/apoHDL$_3$, which are the same within experimental error. Thus, the monolayer–core interactions appear to have no effect upon the rate of segmental motions. However, the values obtained at 25 °C ($\simeq$34 ms) are significantly different from the value of $\simeq$60 ms observed at the same temperature for $\simeq$2.5 mol % [$^2H_6$]TO incorporated into egg PC liposomes (Gorrissen et al., 1982).

In the case of native HDL, which contains triglycerides, the dynamic behavior of the cholesteryl esters has been found to be comparable to cholesteryl ester/triglyceride mixtures by ^{13}C NMR measurements (Hamilton & Cordes, 1978). However, both the present study and that of Parmar et al. (1983) demonstrate that cholesteryl esters in HDL can possess considerable motions in the absence of triglyceride, which we attribute largely to interactions with surface phospholipid.

Although the results from [$^2H_3$]CO/egg PC/apoHDL$_3$ and [$^2H_6$]TO/egg PC/apoHDL$_3$ cannot be directly extrapolated to native HDL because of the simplicity of the model systems, the fatty acid composition of the phospholipid monolayers is similar (Scanu, 1979; Forrest, 1977). Therefore, it is possible that the existence of a state of disordered ester in native HDL above 0 °C (Tall et al., 1977; Jonas & Jung, 1975) can be partly explained on the basis of monolayer–core interactions. The greater compositional heterogeneity of the native system will also contribute to the disordering. Further studies using more complicated model systems are necessary to clarify this point.

Effect of Core on Monolayer. The effect of different core components on the phospholipid monolayer was studied by comparing the temperature dependence of the ^2H NMR line widths of [$^2H_2$]PC in [$^2H_2$]PC/CO/apoHDL$_3$ and [$^2H_2$]-PC/TO/apoHDL$_3$. From the ^2H NMR spectra in Figure 6 and the data in Table III, the line widths of [$^2H_2$]PC are seen to be broader at all temperatures in the particles containing CO than in those containing TO. Values of S_{CD} as a function of temperature are given in Table III for [$^2H_2$]PC/CO/apoHDL$_3$ and [$^2H_2$]PC/TO/apoHDL$_3$, and a plot of S_{CD} versus T is given in Figure 7. The order parameter S_{CD} was determined from eq 14, using a value of $D = 2 \times 10^{-8}$ cm^2/s in the calculation. Values of $D = (1.9 \pm 0.3) \times 10^{-8}$ cm^2/s and $D = (1.8 \pm 0.3) \times 10^{-8}$ cm^2/s have been determined for phospholipids in HDL$_2$ using ^2H and ^{31}P NMR, respectively, and a value of $D = (2.3 \pm 0.8) \times 10^{-8}$ cm^2/s has been determined for HDL$_3$ using ^{31}P NMR (Cushley et al., 1987). We have also estimated the order parameter for [$^2H_2$]PC/CO/apoHDL$_3$ at several temperatures by simulating a super-Lorentzian line shape based upon the particle size distribution for different values of S_{CD}, as described by Parmar et al. (1984). These values were found to be ≤5% higher than the single Lorentzian estimates, which is within the limit of ±10% error in line width. Hence, we have used the S_{CD} values obtained from eq 14.

The values of S_{CD} = 0.39 and 0.33 obtained for [$^2H_2$]-PC/CO/apoHDL$_3$ and [$^2H_2$]PC/TO/apoHDL$_3$ rHDLs, respectively, at 25 °C, agree quite well with the values determined for native HDLs at approximately the same temperature. Values of S_{CD} = 0.37 (Parmar et al., 1985) and 0.30 (Parmar, 1985) were obtained for ≤5 mol % of [5,5,6,6-$^2H_4$]palmitic acid incorporated into the monolayer of native HDL$_3$ and HDL$_2$, respectively. The deuterium T_1 values we obtained for [$^2H_2$]PC/CO/apoHDL$_3$ (16 ms) and [$^2H_2$]-PC/TO/apoHDL$_3$ (14 ms) rHDLs (Table I) are also in close agreement with the values obtained for HDL$_3$ (16 ms) and HDL$_2$ (15 ms). Thus, the orientational order and relaxation rates of the phospholipid monolayer in the [$^2H_2$]PC/CO/apoHDL$_3$ and [$^2H_2$]PC/TO/apoHDL$_3$ systems at 25 °C are essentially identical with the native systems. This further supports the use of simple model systems to elucidate properties of native lipoproteins.

The order parameters of [$^2H_2$]PC in both [$^2H_2$]PC/CO/apoHDL$_3$ and [$^2H_2$]PC/TO/apoHDL$_3$ decrease with increasing temperature, with the values of [$^2H_2$]PC/CO/apoHDL$_3$ being larger over the entire temperature range (Figure 7). Over the range of −5 to 45 °C, neat CO is a solid while neat TO is a liquid. Thus, we assume that CO in rHDL would be more ordered than TO at any given temperature. The larger values of S_{CD} observed with [$^2H_2$]PC/CO/apoHDL$_3$ are then due to interactions of the PC acyl chains with the more ordered CO core.

Although there may be too few molecules of each core component to form solid or liquid-crystalline phases as found with neat components, some ordering of the core components (greater for CO than for TO) is expected on the basis of our previous work with rHDL, in which considerable ordering of cholesteryl palmitate was observed (Parmar et al., 1983). The possibility of protein–lipid interactions contributing to the differential temperature behavior of [$^2H_2$]PC in [$^2H_2$]PC/CO/apoHDL$_3$ and [$^2H_2$]PC/TO/apoHDL$_3$ rHDLs seems unlikely since apoHDL$_3$ are surface proteins (Morrisett et al., 1977) and in both cases the phospholipid is identical. Hence, the effects observed must originate from interactions with the core.

It is of considerable interest that the monolayer–core interaction is observable as far up the PC chain as the 5,5-position. In order to determine whether the influence of the different cores of [$^2H_2$]PC/CO/apoHDL$_3$ and [$^2H_2$]PC/TO/apoHDL$_3$ extended to the head-group region of the particles, ^{31}P NMR spectra of the rHDLs were recorded at 25 and 6 °C, and the line widths are given in Table III. The line widths of the two samples were essentially identical at each temperature; i.e., no differential effects originating from the

core components were observed. The line widths were slightly broader at 6 °C, however, ($\simeq$73 Hz compared to $\simeq$60 Hz at 25 °C).

The presence of ordered PC in rHDLs, especially at low temperatures, is clearly indicated by the order parameter measurements in Table III and Figure 7. The maximum possible value of $|S_{CD}|$ for phospholipids is 1. The value of $\simeq$0.77 observed for [$^2H_2$]PC in [$^2H_2$]PC/CO/apoHDL$_3$ between −5 and 2.5 °C indicates that at the 5,5-position of the acyl chains, the PC is highly ordered. As the temperature is increased, S_{CD} decreases until $\simeq$25 °C and then levels off at $\simeq$0.37. Over the temperature range studied, the order parameter versus temperature curve for [$^2H_2$]PC/CO/apoHDL$_3$ is sigmoidal, whereas the [$^2H_2$]PC/TO/apoHDL$_3$ curve shows a smooth decrease with temperature. While the midpoint of the [$^2H_2$]PC/CO/apoHDL$_3$ curve of $\simeq$18 °C is very much less than the melting temperature of either DPPC multilamellar dispersions (42 °C) or neat CO (51 °C), large melting point depressions have been observed in other systems. For example, incorporation of $\simeq$5 wt % cholesteryl *cis*-parinarate into the core of LDL results in a 10–15 °C depression in the T_m of the core esters (Sklar et al., 1982). Since ^2H NMR is more sensitive to changes in motional rates than bulk techniques such as DSC (Meier et al., 1983; Thewalt et al., 1986), it is possible that we are seeing small changes in cooperative motions of the phospholipids in [$^2H_2$]PC/CO/apoHDL$_3$. Clearly, the order of the PC decreases with increasing temperature, with the shapes of the curves and the magnitude of the S_{CD} values influenced by the order of the core components.

The interactions observed between core and monolayer in the present study are maximal at low temperatures (Figures 3, 5, and 7). Above 25 °C, the line widths of the core lipids are the same within experimental error whether egg PC or DPPC is present in the monolayer. However, S_{CD} of [$^2H_2$]PC is seen to be higher in rHDLs containing CO than in those containing TO at temperatures as high as 45 °C (Figure 7), indicating that core–monolayer interactions are detected at physiological temperatures.

The results from the current study demonstrate that lipid–lipid interactions occur between the core components and the phospholipid acyl chains of the monolayer in HDL. Increasing (or decreasing) the order in one domain was found to result in increased (or decreased) order in the other. Effects of the core on the monolayer can be observed at least as high as the 5,5-position of the PC acyl chains. The results are consistent with a structure of HDL wherein interdigitation of core and monolayer components occurs, i.e., a model in which the core and monolayer are not separated by a distinct boundary. Nevertheless, further studies are necessary to clarify the mechanism of core–monolayer interactions and to see whether these observations extend to the other classes of lipoproteins.

REFERENCES

Abragam, A. (1961a) *The Principles of Nuclear Magnetism*, pp 232–236, Clarendon, Oxford.

Abragam, A. (1961b) *The Principles of Nuclear Magnetism*, pp 424–427, Clarendon, Oxford.

Ames, B. N. (1966) *Methods Enzymol. 8*, 115.

Baumstark, M., Welte, W., & Kreutz, W. (1983) *Biochim. Biophys. Acta 751*, 108–120.

Bloom, M., & Smith, I. C. P. (1985) in *Progress in Protein–Lipid Interactions* (Watts, A., & De Pont, J. J. H. H. M., Eds.) Vol. 1, pp 61–88, Elsevier, New York.

Brainard, J. R., Knapp, R. D., Patsch, J. R., Gotto, A. M., & Morrisett, J. D. (1980) *Ann. N.Y. Acad. Sci. 348*, 299–317.

Burnett, L. J., & Muller, B. H. (1971) *J. Chem. Phys. 55*, 5829–5831.

Carew, T. E., Hayes, S. B., Koschinsky, T. K., & Steinberg, D. (1976) *Lancet 1*, 1315–1317.

Cullis, P. R. (1976) *FEBS Lett. 70*, 223–228.

Cushley, R. J., Treleaven, W. D., Parmar, Y. I., Chana, R. S., & Fenske, D. B. (1987) *Biochem. Biophys. Res. Commun. 146*, 1139–1145.

Davis, J. H. (1983) *Biochim. Biophys. Acta 737*, 117–171.

Finer, E. G., Henry, R., Leslie, R. B., & Robertson, R. N. (1975) *Biochim. Biophys. Acta 380*, 320–337.

Forrest, B. J. (1977) Ph.D. Thesis, Simon Fraser University.

Forte, G. M., Nichols, A. V., & Glaeser, R. M. (1968) *Chem. Phys. Lipids 2*, 396–398.

Goldstein, J. L., & Brown, M. S. (1977) *Annu. Rev. Biochem. 46*, 897–930.

Gorrissen, H., Tulloch, A. P., & Cushley, R. J. (1982) *Chem. Phys. Lipids 31*, 245–255.

Grover, A. K., & Cushley, R. J. (1979) *J. Labelled Compd. Radiopharm. 16*, 307–313.

Hamilton, J. A., & Cordes, E. H. (1978) *J. Biol. Chem. 253*, 5193–5198.

Hamilton, J. A., Talkowski, C., Childers, R. F., Williams, E., Allerhand, A., & Cordes, E. H. (1974) *J. Biol. Chem. 249*, 4872–4878.

Havel, R. J., Elders, H. A., & Bragdon, J. H. (1955) *J. Clin. Invest. 34*, 1345–1353.

Henderson, T. O., Kruski, A. W., Davis, L. G., Glonek, T., & Scanu, A. M. (1975) *Biochemistry 14*, 1915–1920.

Hirz, R., & Scanu, A. M. (1970) *Biochim. Biophys. Acta 207*, 364–367.

Jonas, A., & Jung, R. W. (1975) *Biochem. Biophys. Res. Commun. 66*, 651–657.

Laemmli, U. K. (1970) *Nature (London) 227*, 680–685.

Laggner, P., & Muller, K. W. (1978) *Q. Rev. Biophys. 11*, 371–425.

Lowry, O. H., Rosebrough, N. J., Farr, A. L., & Randall, R. J. (1951) *J. Biol. Chem. 193*, 265–275.

Lund-Katz, S., & Phillips, M. C. (1981) *Biochem. Biophys. Res. Commun. 100*, 1735–1742.

Meier, P., Ohmes, E., Kothe, G., Blume, A., Weidner, J., & Eibl, H.-J. (1983) *J. Phys. Chem. 87*, 4904–4912.

Miller, G. J., & Miller, N. E. (1975) *Lancet 1*, 16–19.

Morrisett, J. D., Jackson, R. L., & Gotto, A. M., Jr. (1977) *Biochim. Biophys. Acta 472*, 93–133.

Parmar, Y. I. (1985) Ph.D. Thesis, Simon Fraser University.

Parmar, Y. I., Gorrissen, H., Wassall, S. R., & Cushley, R. J. (1983) *J. Biol. Chem. 258*, 2000–2004.

Parmar, Y. I., Wassall, S. R., & Cushley, R. J. (1984) *J. Am. Chem. Soc. 106*, 2434–2435.

Parmar, Y. I., Gorrissen, H., Wassall, S. R., & Cushley, R. J. (1985) *Biochemistry 24*, 171–176.

Ritter, M. C., & Scanu, A. M. (1977) *J. Biol. Chem. 252*, 1208–1216.

Scanu, A. M. (1979) in *The Biochemistry of Atherosclerosis* (Scanu, A. M., Wissler, R. W., & Getz, G. S., Eds.) pp 3–8, Marcel Dekker, New York.

Scanu, A. M., Toth, J., Edelstein, C., Koga, S., & Stiller, E. (1969) *Biochemistry 8*, 3309–3316.

Shen, B. W., Scanu, A. M., & Kezdy, F. J. (1977) *Proc. Natl. Acad. Sci. U.S.A. 74*, 837–841.

Sklar, L. A., Mantulin, W. W., & Pownall, H. J. (1982) *Biochem. Biophys. Res. Commun. 105*, 674–680.

Smith, L. C., Pownall, H. J., & Gotto, A. M., Jr. (1978) *Annu. Rev. Biochem. 47*, 751–777.
Stein, O., & Stein, Y. (1976) *Biochim. Biophys. Acta 431*, 363–368.
Stockton, G. W., Polnaszek, C. F., Tulloch, A. P., Hasan, F., & Smith, I. C. P. (1976) *Biochemistry 15*, 954–966.
Tall, A. R. (1980) *Ann. N.Y. Acad. Sci. 348*, 335–351.
Tall, A. R., & Small, D. M. (1979) *Adv. Lipid Res. 17*, 1–51.
Tall, A. R., Deckelbaum, R. J., Small, D. M., & Shipley, G. G. (1977) *Biochim. Biophys. Acta 487*, 145–153.
Thewalt, J. L., Wassall, S. R., Gorrissen, H., & Cushley, R. J. (1985) *Biochim. Biophys. Acta 817*, 355–365.
Thewalt, J. L., Tulloch, A. P., & Cushley, R. J. (1986) *Chem. Phys. Lipids 39*, 93–107.
Treleaven, W. D., Parmar, Y. I., Gorrissen, H., & Cushley, R. J. (1986) *Biochim. Biophys. Acta 877*, 198–210.
Valic, M. I., Gorrissen, H., Cushley, R. J., & Bloom, M. (1979) *Biochemisty 18*, 854–859.
Verdery, R. B., III, & Nichols, A. V. (1975) *Chem. Phys. Lipids 14*, 123–134.
Wassall, S. R., Treleaven, W. D., Parmar, Y. I., & Cushley, R. J. (1982) *Biochem. Biophys. Res. Commun. 107*, 429–434.
Zilversmit, D. B. (1984) *J. Lipid Res. 25*, 1563–1569.

Apolipoproteins C-I, C-II, and C-III: Kinetics of Association with Model Membranes and Intermembrane Transfer†

Barry J. McKeone,* John B. Massey, Roger D. Knapp, and Henry J. Pownall
Department of Internal Medicine, Baylor College of Medicine, and The Methodist Hospital, 6565 Fannin Street, MS A601, Houston, Texas 77030

Received September 23, 1987; Revised Manuscript Received February 10, 1988

ABSTRACT: The apoproteins (apo) C-I, C-II, and C-III are low molecular weight amphiphilic proteins that are associated with the lipid surface of the plasma chylomicron, very low density lipoprotein (VLDL), and high-density lipoprotein (HDL) subfractions. Purified apoC-I spontaneously reassociates with VLDL, HDL, and single-bilayer vesicles (SBV) of 1-palmitoyl-2-oleoyl-*sn*-glycero-3-phosphocholine. ApoC-I also transfers reversibly from VLDL to HDL and from VLDL and HDL to SBV. The kinetics of association of the individual apoC proteins with SBV are second order overall and first order with respect to lipid and protein concentrations. At 37 °C, the rates of association were 2.5×10^{10}, 4.0×10^{10} and 3.8×10^{10} M^{-1} s^{-1} for apoC-I, apoC-II, and apoC-III, respectively. Arrhenius plots of association rate vs temperature were linear and yielded activation energies of 11.0 (apoC-I), 9.0 (apoC-II), and 10.6 kcal/mol (apoC-III). The kinetics of vesicle to vesicle apoprotein transfer are biexponential for intermembrane transfer, indicating two concurrent transfer processes. Rate constants at 37 °C for the fast component of dissociation were 11.7, 9.5, and 9.9 s^{-1}, while rate constants for the slow component were 1.3, 0.6, and 0.9 s^{-1} for apoC-I, apoC-II, and apoC-III, respectively. The dissociation constants, K_d, of apoC-I, apoC-II, and apoC-III bound to the surface monolayer of phospholipid-coated latex beads were 0.5, 1.4, and 0.5 μM, respectively. These studies show that the apoC proteins are in dynamic equilibrium among phospholipid surfaces on a time scale that is rapid compared to lipolysis, lipid transfer, and lipoprotein turnover.

The C apolipoproteins, apoC-I, apoC-II, and apoC-III, are low molecular weight proteins of known sequence derived from the high-density lipoprotein (HDL),[1] very low density lipoprotein (VLDL), and chylomicron subfractions of the plasma lipoproteins [for a review, see Mahley et al. (1984)]. The main source of apoC proteins in plasma appears to be the liver, although some synthesis may occur in the intestine (Krause et al., 1981). The apoC proteins stabilize lipoprotein structure (Morrisett et al., 1977) and in part regulate their catabolism. ApoC-I activates the enzyme lecithin:cholesterol acyltransferase in vitro (Soutar et al., 1975); apoC-II has been shown to activate extrahepatic lipoprotein lipase (Breckenridge et al., 1978). Though its role is less clear, apoC-III may regulate uptake of chylomicron remnants by the liver (Shelburne et al., 1980). The apoC proteins are in dynamic equilibrium among the lipoprotein classes and subclasses (Eisenberg et al., 1979). In the lipolytic cascade that begins with VLDL, the apoC proteins transfer spontaneously from VLDL to HDL (Berman et al., 1978). Newly secreted VLDL subsequently acquires its complement of apoC proteins from circulating HDL (Wu & Windmueller, 1979). The size, surface properties, and chemical composition of the lipoproteins have a role in determining the distribution of the apoC proteins between density classes (Patsch et al., 1978). To quantitatively define the regulatory factors that control distribution of apoC proteins and their respective roles in lipoprotein catabolism, it is important to understand the underlying mechanisms of protein–lipid association. Herein, we report on the thermodynamics and mechanisms by which the apoC proteins distribute among model lipoproteins.

† This research was supported by grants from the National Institutes of Health (HL 27341, HL 30913, HL 30914, and T32-HL 07582).

[1] Abbreviations: PC, phosphatidylcholine; POPE, 1-palmitoyl-2-oleoyl-*sn*-glycero-3-phosphoethanolamine; POPC, 1-palmitoyl-2-oleoyl-*sn*-glycero-3-phosphocholine; VLDL, very low density lipoprotein; HDL, high-density lipoprotein; dansyl-PE or DPE, dansyl [8-(dimethylamino)-1-naphthalenesulfonate] derivative of POPE; SBV, single-bilayer vesicle(s); Tris-HCl, tris(hydroxymethyl)aminomethane hydrochloride; EDTA, ethylenediaminetetraacetic acid.

0006-2960/88/0427-4500$01.50/0